Two-Dimensional Dion-Jacobson Structure Perovskites for Efficient Sky-Blue Light-Emitting Diodes

*Yuqiang Liu, Luis K. Ono, Guoqing Tong, Hui Zhang, Yabing Qi**

Energy Materials and Surface Sciences Unit (EMSSU), Okinawa Institute of Science and Technology Graduate University (OIST), Okinawa 904-0495, Japan

*Corresponding author: Yabing.Qi@OIST.jp (Y. B. Q.).

Abstract:

Two-dimensional Ruddlesden-Popper (RP) and Dion-Jacobson (DJ) phase perovskites are promising alternatives to fabricate blue perovskite light-emitting diodes (PeLEDs) due to their strong quantum/dielectric confinement. While the RP phase perovskites have been widely used as emitter layers in blue PeLEDs, the DJ phase perovskites, possessing better structural stability and charge transfer property, have received little attention. Here, we reported the use of DJ phase perovskites for fabricating efficient sky-blue PeLEDs. Organic diamine propane-1,3-diammonium cations were firstly incorporated into $CsPbBr_3$ to prepare DJ phase perovskites. RbBr was further incorporated as a passivation agent to eliminate traps. It is found that diamine cations and RbBr are inter-dependent in terms of increasing the utilization of charges. Radiative recombination is enhanced effectively benefited from the synergetic confinement and passivation effects. The photoluminescence quantum yield approaches 70%. Finally, the fabricated PeLEDs achieved an external quantum efficiency of 8.5% with an emission peak at 490 nm.

TOC Graphic

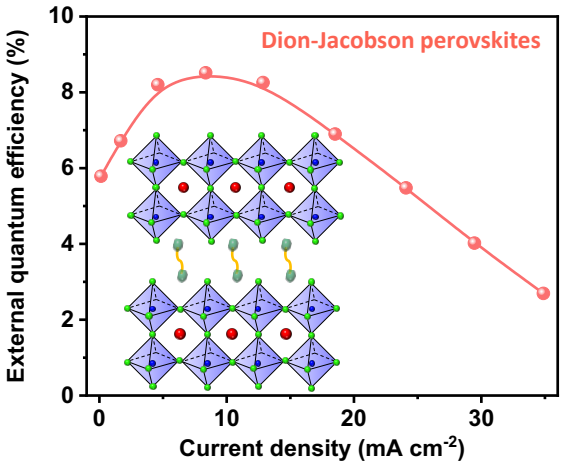
Dion-Jacobson perovskites
External quantum efficiency (%)
Current density (mA cm-2)
0
2
4
6
8
10
0
10
20
30

Perovskite materials possess attractive optoelectronic properties and are promising candidates in the field of displays and light sources.[1-4] Since the first room-temperature perovskite light-emitting diode (PeLED) was reported,[5] impressive advances have been made in PeLEDs.[6-8] State-of-the-art external quantum efficiencies (EQEs) exceeding 20% have been realized in green, red, and near-infrared PeLED devices.[9-11] However, the efficiency of blue PeLEDs still lags, due to adverse issues such as the presence of a large density of traps, spectral instability, and improper charge injection barriers.[12, 13] Several perovskite compositions and structures (e.g., mixed chloride/bromide compositions and low-dimensional structures) have been intensively studied to address these issues in blue PeLEDs.[14-17] Among these new approaches, two-dimensional (2D) perovskites with strong quantum and/or dielectric confinement effects provide a facile strategy towards efficient blue PeLEDs.[18, 19]

The typical 2D perovskites can be categorized into Ruddlesden-Popper (RP), Dion-Jacobson (DJ), and alternating cation (ACI) phases,[20] among which the RP phase is the most studied one in blue PeLEDs currently.[18] Incorporating bulky organic monoamine cations into 3D perovskites is a simple strategy to form RP phases. Lee and coworkers successfully presented the prospect that quasi-2D phase perovskites are favorable for achieving efficient PeLEDs.[21] Encouraging efficiencies have been achieved in blue PeLEDs via tailoring the RP phase compositions.[22-25] For instance, through incorporating phenylbutylammonium cations into 3D perovskites to form quasi-2D phase perovskites, whose EQEs up to 9.5% were obtained for blue PeLEDs with the electroluminescence (EL) peak at 483 nm.[24] On the basis of composition

engineering in 2D $PEA_2(CsPbBr_3)_2PbBr_4$ perovskites (PEA: phenylethylammonium), a champion EQE of 12.1% was realized in blue PeLEDs with the EL peak at 488 nm.[25] However, because of the weak van der Waals interaction between organic cations in RP phases, the adjacent lead halide octahedra $[PbBr_6]^{4-}$ slabs have the inherent tendencies for dissociation, causing the decomposition of perovskites. [26, 27] It is well established that DJ phases formed by incorporating diamine cations provide more stable perovskite structures because the adjacent lead halide slabs are bridged by diamine molecules, instead of the van der Waals interaction.[20] Meanwhile, DJ phase structures possess shorter distances between two adjacent lead halide slabs than those of RP phases, leading to more efficient charge transfer in perovskite devices.[26, 27] But currently little attention has been paid to PeLEDs based on the DJ phase perovskites.

In this work, we report efficient sky-blue PeLEDs using 2D DJ phase perovskites as emitter layers. Organic diamine propane-1,3-diammonium (PDA) cations were incorporated into $CsPbBr_3$ lattice structures to form the DJ phase PDA-$CsPbBr_3$ perovskites. Perovskite films were demonstrated to show tunable emission from green to blue regions with enhanced photoluminescence quantum yield (PLQY) benefited from the quantum/dielectric confinement and passivation effects. Furthermore, by introducing RbBr as passivation agents to eliminate the trap states, nonradiative recombination losses are suppressed effectively. Finally, an EQE of 8.5% was obtained in PeLEDs with an emission peak at 490 nm.

The perovskite films are prepared by spin-coating the precursor solutions of CsBr, $PbBr_2$, and $PDABr_2$ in dimethyl sulfoxide (see Experimental Section), where PDA

cations induce the formation of DJ phases. As shown in Figure 1a of DJ phase perovskites, PDA cations are incorporated into the lattice of $CsPbBr_3$ crystals and connect the adjacent octahedra $[PbBr_6]^{4-}$ slabs through hydrogen bonding.[28, 29] The divalent diamine component of PDA cations ensures that the adjacent slabs are bridged by PDA cations directly, and it is different from RP phases requiring extra van der Waals interaction to maintain the perovskite structures as shown in Figure S1 of the structural difference between RP and DJ phases. The insulating PDA cations serve as spacers on both sides of the $[PbBr_6]^{4-}$ slabs, which form the quantum well structure.[18] Compared with the ineffective utilization of injected charges in 3D perovskites (Figure 1b), these quantum wells in 2D perovskites confine the injected charges to form excitons, as shown in Figure 1c, increasing the utilization of charges.[7] In other words, the DJ phase perovskites can enhance the radiative recombination efficiency of excitons. Detailed characteristics are discussed in the following section.

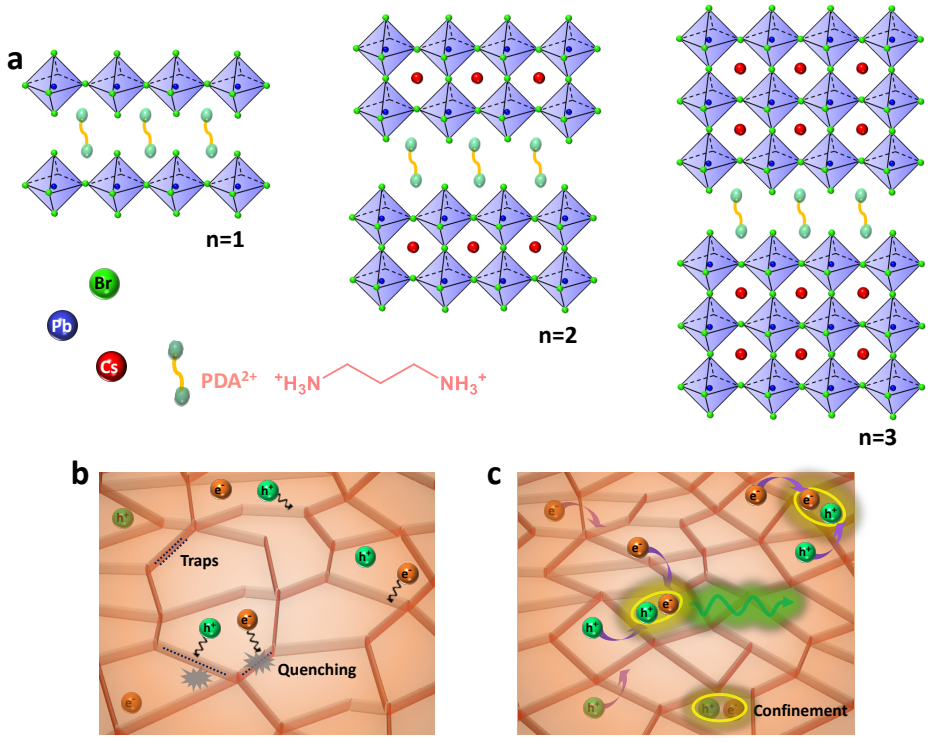

Figure 1. (a) Schematic illustration of the 2D DJ phase perovskites with a layer number (n) of 1, 2, and 3. (b) Charges migration among 3D perovskite domains and quenching at grain boundaries. (c) Excitons confinement and funnel from smaller n to larger n phases in DJ phase perovskites.

The spatial distribution of elements (Figure S2) mapped by energy-dispersive X-ray (EDX) exhibits that N elements (corresponding to PDA cations) are uniformly distributed in the perovskite films. The absorption spectra (Figure S3a) of the perovskite films demonstrate blue-shift tendencies as the $PDABr_2$ ratio increases. The blue shifting is originated from the confinement effects of the 2D phases, i.e., the structural change of perovskites from 3D $CsPbBr_3$ phases to 2D PDA-$CsPbBr_3$ phases.[28, 29] The steady-state photoluminescence (PL) peaks also exhibit blue shifting tendencies, as shown in Figure S3b. PL peaks change from the green color of 521 nm to the blue one of 469 nm upon increasing the $PDABr_2$ ratios from 0 to 0.16 M. Additionally, the steady-state PL intensity of 2D phase perovskite films is stronger than that of 3D ones. As shown in Figure 2a, PL intensity enhancement by 3.4 times is realized upon incorporating 0.06 M $PDABr_2$ in comparison to the intensity of 3D $CsPbBr_3$ perovskite films. When the incorporating ratio of $PDABr_2$ reaches 0.12 M, the PL intensity is over eight times that of the 3D $CsPbBr_3$ one. The enhanced PL intensity proves more effective utilization of charges, which is also evidenced by the average PL lifetimes and PLQY characteristics of the perovskite films. The average PL lifetimes (based on biexponential fitting, Figure 2b) of the perovskite films are 6.4 ns, 11.4 ns, 12.3 ns, 13.3 ns, 19.0 ns, 11.9 ns, and 8.5

ns, corresponding to the $PDABr_2$ ratio of 0 M (i.e., 3D $CsPbBr_3$), 0.06 M, 0.08 M, 0.10 M, 0.12 M, 0.14 M, and 0.16 M, respectively. When 0.12 M $PDABr_2$ is incorporated, the average PL lifetime of the perovskite films is three times that for the 3D $CsPbBr_3$ one. As shown in Figure 2c, the PLQY of the perovskite films is increased to 40.1% after incorporating 0.12 M $PDABr_2$, which is dramatically larger than the value of the 3D $CsPbBr_3$ below 1%.

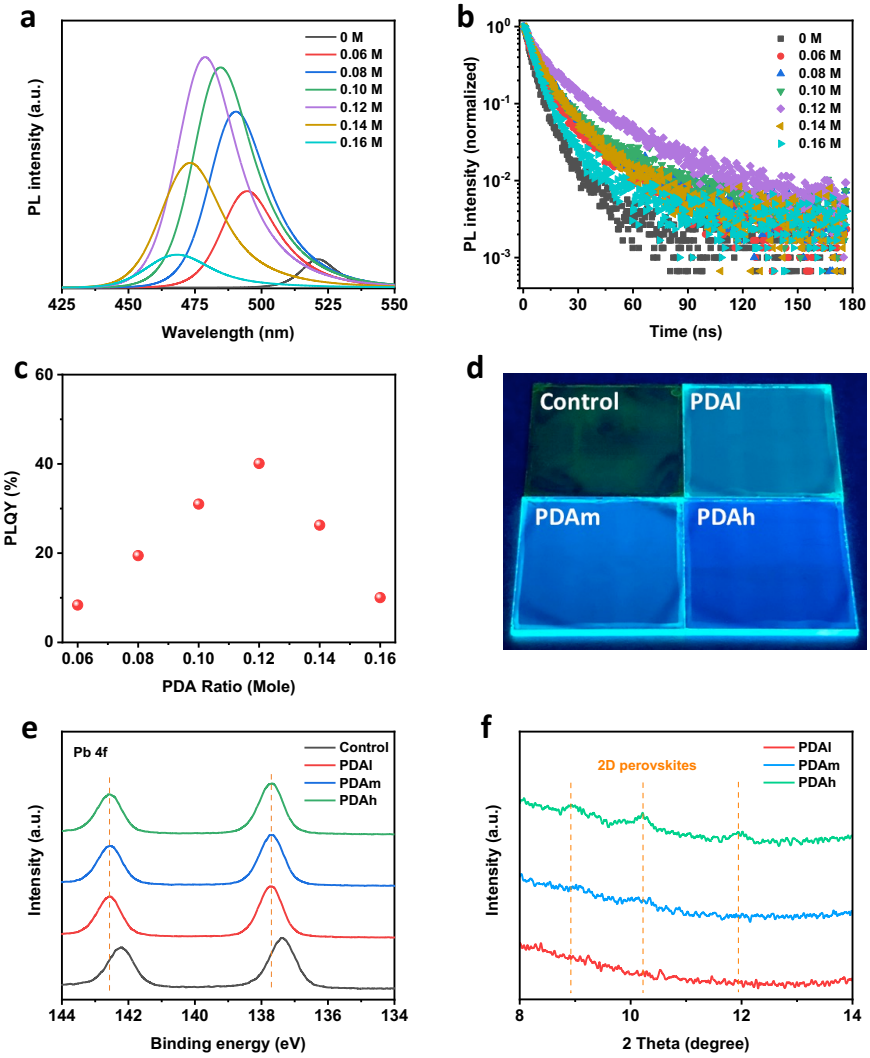

Figure 2. (a) Steady-state PL spectra, (b) time-resolved PL spectra, and (c) PLQY of the perovskite films as a function of the $PDABr_2$ ratio. (d) Photograph of the perovskite films excited under 365 nm ultraviolet radiation. (e) XPS curves of the Pb $4f_{7/2}$ and Pb

4f $_{5/2}$ core levels of the perovskite films. (f) XRD patterns of the perovskite films.

Four different $PDABr_2$ ratios, including 0 M (control), 0.08 M (PDAl), 0.10 M (PDAm), and 0.12 M (PDAh), were used for further investigations. Figure 2d provides photographs of the perovskite films excited under ultraviolet light, where the illumination colors change from green to blue regions. The film morphology is characterized by scanning electron microscope (SEM) images, as shown in Figure S4. Compared with the discontinuous morphology of the 3D $CsPbBr_3$ film, compact films are formed in all PDAl, PDAm, and PDAh films. The compact film morphology is helpful to eliminate the charge losses leaked from these pinholes. X-ray photoelectron spectroscopy (XPS) results of the 2D perovskite films (Figure S5) indicate the existence of the N element from the amine groups of the PDA cations. Furthermore, the core levels of Pb *4f* $_{7/2}$ and Pb *4f* $_{5/2}$ of the perovskite films shift toward higher binding energy values (Figure 2e), which indicates the stronger interaction between Pb^{2+} and PDA cations.[30] X-ray diffraction (XRD) was carried out to investigate the crystallinity of the perovskite films without and with $PDABr_2$. According to the XRD patterns in Figure S6a, the control film demonstrates diffraction peaks at 15.2° and 30.7°, which match well with the (100) and (200) planes in the typical 3D $CsPbBr_3$ perovskites. In parallel, the diffraction peak of (200) plane shifts to a lower diffraction angle of 30.1° after the incorporation of $PDABr_2$ (Figure S6b). The peak shifting means the formation of layered perovskites in the PDA incorporated films.[31] The diffraction peaks of 3D perovskites also decreased, because the 3D phase perovskites change into 2D phase

ones when PDA cations are incorporated, as shown in the SEM images in Figure S4. Meanwhile, the average crystallite sizes of PDA based perovskite films were extracted by the Scherrer equation from (200) peaks. The crystallite sizes of PDAl, PDAm, and PDAh perovskites are approximately 15 nm, which is much smaller than that of 3D perovskites. Meanwhile, as shown in Figure 2f, three new peaks corresponding to 2D perovskites appear at low diffraction angles of the XRD patterns, evidencing the formation of 2D perovskites after incorporating $PDABr_2$. PDAh films show the strongest diffraction intensity, which suggests that PDA cations are favorable for the formation of 2D perovskites.

Although the confinement effects in DJ phase perovskites enlarge the binding energy of charges, trap-assisted nonradiative recombination loss still limits the efficiency of blue PeLEDs. RbBr is introduced into the DJ phase perovskites to address the issue of adverse nonradiative recombination losses. PDAl-Rb, PDAm-Rb, and PDAh-Rb represent PDAl, PDAm, and PDAh with RbBr, respectively. XPS curves in Figure S7 display the existence of Rb elements. Meanwhile, the core levels of Rb *3d* shift toward lower binding energy after being incorporated into perovskites because of the interaction between the RbBr and DJ phase perovskites. The XRD pattern of the PDAl and PDAl-Rb perovskite films are shown in Figure S8 (a). According to the XRD patterns, the diffraction intensity of a 2D peak is hard to be observed. This is because of the relatively low ratio of PDA cations. Hence, PDAh and PDAh-Rb films are used to observe the XRD changes, as shown in Figure S8 (b). According to the XRD patterns of the 2D PDAh and PDAh-Rb films, the diffraction intensity of a 2D peak is enhanced

significantly. Therefore, RbBr is helpful to enhance the ordered arrangement of 2D phases, facilitating the exciton transfer from smaller n to larger n phases in DJ perovskites films.[22] As shown in the steady-state PL spectra in Figure 3a, there is a slight blue shift after incorporating RbBr. However, the radiative recombination efficiency is increased obviously according to PL lifetimes and PLQY results. As shown in Figure 3b, the average PL lifetimes of PDAl-Rb, PDAm-Rb, and PDAh-Rb reach 25.5 ns, 29.2 ns, 21.8 ns, respectively. Compared with those of PDAl (12.3 ns), PDAm (13.3 ns), and PDAh (19.0 ns), the maximum PL lifetime of the perovskite film with RbBr is enhanced by over 50% than that without RbBr. The increase of PL lifetime suggests that RbBr can passivate traps in perovskite films, which results in the increased radiative recombination efficiency of charges.[32] The enhanced PLQY further verifies the passivation effect of RbBr, as shown in Figure S9b. The maximum PLQY of perovskite films with RbBr (PDAm-Rb) reaches 68.8%, which is 70% higher when compared with the PLQY value without RbBr (40.1%).

Furthermore, as shown in the results of the PL intensities and PLQYs (Figure S9), the champion PL performance of perovskite films with RbBr is obtained when the $PDABr_2$ ratio is 0.10 M (PDAm-Rb). However, this ratio is different from the optimized one of 0.12 M (PDAh), when there are no RbBr agents (Figure 2a and 2c). Additionally, the passivation effect of RbBr is more obvious when the $PDABr_2$ ratio is below 0.12 M. Once the $PDABr_2$ ratio is over 0.12 M, RbBr does not show a noticeable effect in the PL performance of the perovskite films. In other words, the passivation effects of $PDABr_2$ and RbBr are inter-dependent. Schematic illustrations are depicted to present

the detailed analyses, as shown in Figure 3c-e. Because of the small binding energy in 3D perovskites, injected charges tend to separate and migrate, instead of forming excitons. Meanwhile, defect states at grain boundary trap these excitons and then quench them (Figure 3c).[33] These issues limit the efficiency of radiative recombination. Upon incorporating $PDABr_2$ agents into 3D perovskites, two effects are realized to improve radiative recombination (Figure 3d): the charges are forced to be confined into excitons owing to the enlarged binding energy;[33] the quenching losses are reduced because the traps are passivated by $PDABr_2$ agents.[34] When the incorporating ratio of $PDABr_2$ is below 0.12 M, a higher $PDABr_2$ ratio results in better confinement and passivation effects. However, accompanied by further increasing the ratio to over 0.12 M, the utilization of charges is decreased, indicating that it is hard to eliminate these traps using only $PDABr_2$ agents. Hence, RbBr is utilized as synergetic agents to solve the dilemma to passivate traps, as shown in Figure 3e.

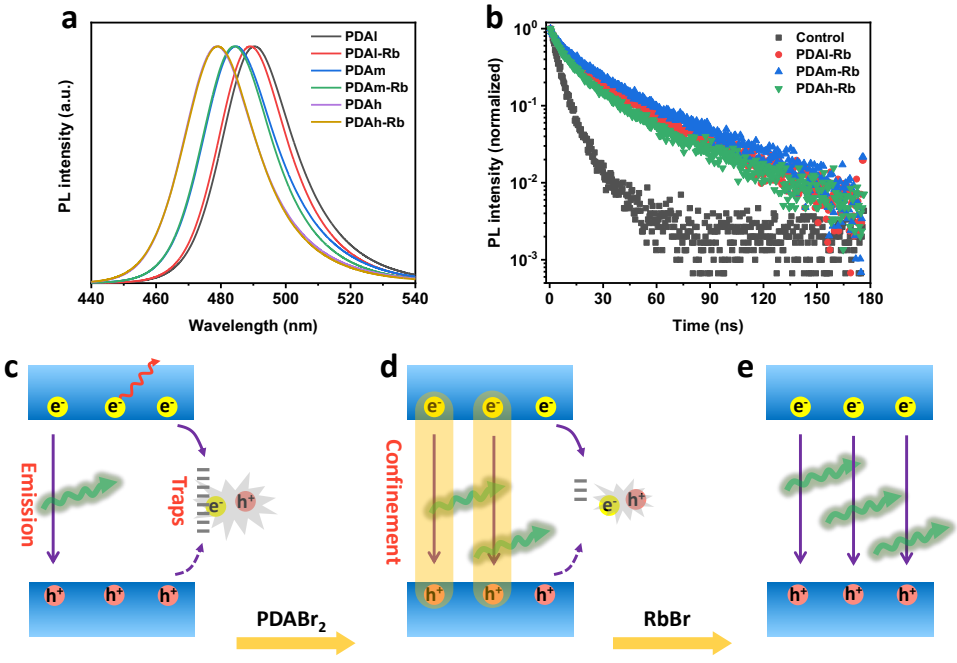

Figure 3. (a) Normalized steady-state PL spectra and (b) time-resolved PL spectra of

perovskite films with and without RbBr. Schematic depicting (c) charges migration and nonradiative recombination, (d) excitons confinement and traps passivation by incorporation of organic molecules of $PDABr_2$, and (e) traps passivation by RbBr.

We fabricated blue PeLEDs using the device structure of indium tin oxide (ITO)/poly(3,4-ethylenedioxythiophene):poly(styrenesulfonate) (PEDOT:PSS)/ perovskites/2,2',2''-(1,3,5-benzenetriyl) tris-(1-phenyl-1Hbenzimidazole) (TPBi)/8-hydroxyquinolinolato-lithium (Liq)/aluminum (Al). The thickness of the perovskite layer is approximately 45 nm, according to the cross-sectional SEM image in Figure S10. According to the ultraviolet photoemission spectroscopy (UPS) results in Figure S11, we can derive the energy level diagram of these devices (Figure 4a). Holes and electrons are injected into perovskite films with the assistance of the PEDOT:PSS and TPBi layer, respectively. As shown in the EL spectra (Figure 4b), when the PDAl-Rb films are used as the emitter layer, EL peaks are located at 490 nm without obvious peak shifting as the bias voltage is increased up to 6 V. The corresponding CIE color coordinates are (0.07, 0.32) as shown in Figure S12. Similar EL spectra at 490 nm are also demonstrated with PDAl as the emitter layers (Figure S13a). However, according to the current density-luminance-voltage curves (Figure 4c), the PDAl-Rb based device presents stronger brightness than the PDAl based ones under the same applied bias voltage. As for the PDAl-Rb based devices, the highest brightness reaches 2257 cd/m^2, which is two times that of the PDAl based one (1039 cd/m^2). EQE values are improved upon the incorporation of RbBr, as shown in Figure 4d. The maximum EQE of PDAl

based devices is 5.1%. With RbBr as the passivation agent, the maximum EQE of PDAl-Rb based PeLEDs reaches 8.5%. Figure S14 is the current efficiency-voltage curves of the PeLEDs. Meanwhile, the electrical characteristics of the devices using different PDA ratios are presented in Figure S15. The EQE of the PeLED reaches 12.4% with an EL peak at 496 nm, when the perovskite films with 0.06 M PDA are used as emitter layers. There is no EL emission from the devices when PDAm, PDAh, PDAm-Rb and PDAh-Rb films serve as emitters. This is possibly because (i) a high PDA ratio enlarges the resistance for charge transport, because of the low charge carrier mobility of 2D phase perovskites and/or (ii) according to the energy level diagram in Figure 4 (a), the injection barrier increases when the PDA ratio increases. As a consequence, charge injection and transport are suppressed, and a large number of charges are lost via Joule heating, instead of radiative recombination. Additionally, when the initial luminance is 100 cd/m^2, the operational half-lifetime of PDAl based device is 109 seconds, as shown in Figure S13b. After introducing RbBr agents, the half-lifetime is enhanced to 3.6 minutes. The EL spectra of the PDAl-Rb based PeLEDs over the period from 0 to 3.6 minutes were shown in Figure S16. The EL peaks are located within 490-491 nm during the operation process, indicating that the PDAl-Rb based PeLEDs possess a stable EL peak during the working period. Because of the trap passivation effect of RbBr, quenching losses of injected charges are reduced, which enhances radiative recombination efficiency and reduces Joule heating, and consequently, both the EQE and half-lifetime performances are improved.[35, 36]

In summary, the 2D DJ phase perovskites are successfully prepared as emitter

layers in sky-blue PeLEDs. Incorporating bulky organic $PDABr_2$ not only tailors the emission peaks toward the blue region but also improves the radiative recombination of charges, because of the confinement and passivation effects. RbBr as synergetic agents further enhances the utilization of charges in DJ phase perovskite films through trap passivation. Finally, an EQE of 8.5% is achieved in sky-blue PeLEDs. However, the deep blue PeLEDs cannot work well when the $PDABr_2$ ratio is over 0.1 M. Therefore, more research is still needed to address these issues.

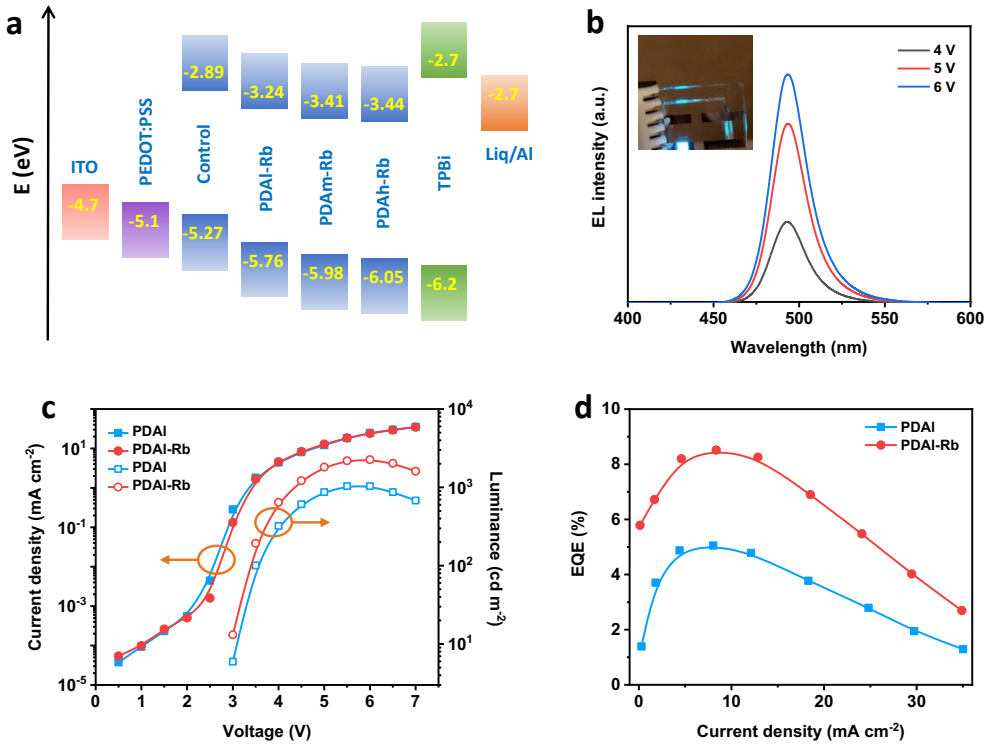

Figure 4. (a) Energy level diagram of PeLEDs. (b) EL spectra of PeLED devices with PDAI-Rb as the emitter layer. The inset optical photography is a PeLED under 4 V bias. (c) Current density-luminance-voltage curves. (d) EQE-current density curves of PeLEDs.

ASSOCIATED CONTENT

Supporting Information

Supporting Information is available: Experimental section; Schematic of RP and DJ phase perovskites; SEM, TEM and EDX mapping of perovskite films; Absorption, steady-state PL spectra and PLQY of perovskite films; XPS spectra of N *1s* and Rb *3d* core levels; XRD patterns of perovskite films; UPS spectra of perovskite films; Electrical performances of devices.

AUTHOR INFORMATION

Corresponding Author

Yabing.Qi@OIST.jp (Y. B. Q.)

Notes

The authors declare no competing financial interest.

ACKNOWLEDGMENTS

This work was supported by funding from the Energy Materials and Surface Sciences Unit of the Okinawa Institute of Science and Technology Graduate University, the OIST R&D Cluster Research Program, and the OIST Proof of Concept (POC) Program. We thank the OIST Micro/Nanofabrication Section and Imaging Section for the support.

REFERENCES

1. Stranks, S. D.; Snaith, H. J. Metal-Halide Perovskites for Photovoltaic and Light-

Emitting Devices. *Nat. Nanotechnol.* **2015**, 10 (5), 391-402.

2. Park, M. H.; Kim, J. S.; Heo, J. M.; Ahn, S.; Jeong, S. H.; Lee, T. W. Boosting Efficiency in Polycrystalline Metal Halide Perovskite Light-Emitting Diodes. *ACS Energy Lett.* **2019**, 4 (5), 1134-1149.

3. Quan, L. N.; Rand, B. P.; Friend, R. H.; Mhaisalkar, S. G.; Lee, T. W.; Sargent, E. H. Perovskites for Next-Generation Optical Sources. *Chem. Rev.* **2019**, 119 (12), 7444-7477.

4. Liu, Y.; Ono, L. K.; Qi, Y. B. Organic Additive Engineering toward Efficient Perovskite Light-Emitting Diodes. *InfoMat.* **2020**, 2 (6), 1095-1108.

5. Tan, Z. K.; Moghaddam, R. S.; Lai, M. L.; Docampo, P.; Higler, R.; Deschler, F.; Price, M.; Sadhanala, A.; Pazos, L. M.; Credgington, D.; Hanusch, F.; Bein, T.; Snaith, H. J.; Friend, R. H. Bright Light-Emitting Diodes Based on Organometal Halide Perovskite. *Nat. Nanotechnol.* **2014**, 9 (9), 687-692.

6. Cho, H.; Jeong, S. H.; Park, M. H.; Kim, Y. H.; Wolf, C.; Lee, C. L.; Heo, J. H.; Sadhanala, A.; Myoung, N.; Yoo, S.; Im, S. H.; Friend, R. H.; Lee, T. W. Overcoming the Electroluminescence Efficiency Limitations of Perovskite Light-Emitting Diodes. *Science* **2015**, 350 (6265), 1222-1225.

7. Wang, N.; Cheng, L.; Ge, R.; Zhang, S.; Miao, Y.; Zou, W.; Yi, C.; Sun, Y.; Cao, Y.; Yang, R.; Wei, Y.; Guo, Q.; Ke, Y.; Yu, M.; Jin, Y.; Liu, Y.; Ding, Q.; Di, D.; Yang, L.; Xing, G.; Tian, H.; Jin, C.; Gao, F.; Friend, R. H.; Wang, J.; Huang, W. Perovskite Light-Emitting Diodes Based on Solution-Processed Self-Organized Multiple Quantum Wells. *Nat. Photonics* **2016**, 10 (11), 699-704.

8. Xiao, Z.; Kerner, R. A.; Zhao, L.; Tran, N. L.; Lee, K. M.; Koh, T.-W.; Scholes, G. D.; Rand, B. P. Efficient Perovskite Light-Emitting Diodes Featuring Nanometre-Sized Crystallites. *Nat. Photonics* **2017**, 11 (2), 108-115.

9. Lin, K.; Xing, J.; Quan, L. N.; de Arquer, F. P. G.; Gong, X.; Lu, J.; Xie, L.; Zhao, W.; Zhang, D.; Yan, C.; Li, W.; Liu, X.; Lu, Y.; Kirman, J.; Sargent, E. H.; Xiong, Q.; Wei, Z. Perovskite Light-Emitting Diodes with External Quantum Efficiency Exceeding 20 Per Cent. *Nature* **2018**, 562 (7726), 245-248.

10. Chiba, T.; Hayashi, Y.; Ebe, H.; Hoshi, K.; Sato, J.; Sato, S.; Pu, Y. J.; Ohisa, S.; Kido, J. Anion-Exchange Red Perovskite Quantum Dots with Ammonium Iodine Salts for Highly Efficient Light-Emitting Devices. *Nat. Photonics* **2018**, 12 (11), 681-687.

11. Xu, W. D.; Hu, Q.; Bai, S.; Bao, C. X.; Miao, Y. F.; Yuan, Z. C.; Borzda, T.; Barker, A. J.; Tyukalova, E.; Hu, Z. J.; Kawecki, M.; Wang, H. Y.; Yan, Z. B.; Liu, X. J.; Shi, X. B.; Uvdal, K.; Fahlman, M.; Zhang, W. J.; Duchamp, M.; Liu, J. M.; Petrozza, A.; Wang, J. P.; Liu, L. M.; Huang, W.; Gao, F. Rational Molecular Passivation for High-Performance Perovskite Light-Emitting Diodes. *Nat. Photonics* **2019**, 13 (6), 418-424.

12. Liu, X. K.; Xu, W.; Bai, S.; Jin, Y.; Wang, J.; Friend, R. H.; Gao, F. Metal Halide Perovskites for Light-Emitting Diodes. *Nat. Mater.* **2021**, 20 (1), 10-21.

13. Fang, T.; Zhang, F.; Yuan, S.; Zeng, H.; Song, J. Recent Advances and Prospects toward Blue Perovskite Materials and Light-Emitting Diodes. *InfoMat.* **2019**, 1 (2), 211-233.

14. Yuan, F.; Ran, C. X.; Zhang, L.; Dong, H.; Jiao, B.; Hou, X.; Li, J. R.; Wu, Z. X. A Cocktail of Multiple Cations in Inorganic Halide Perovskite toward Efficient and

Highly Stable Blue Light-Emitting Diodes. *ACS Energy Lett.* **2020**, 5 (4), 1062-1069.

15. Zhang, B. B.; Yuan, S.; Ma, J. P.; Zhou, Y.; Hou, J.; Chen, X.; Zheng, W.; Shen, H.; Wang, X. C.; Sun, B.; Bakr, O. M.; Liao, L. S.; Sun, H. T. General Mild Reaction Creates Highly Luminescent Organic-Ligand-Lacking Halide Perovskite Nanocrystals for Efficient Light-Emitting Diodes. *J. Am. Chem. Soc.* **2019**, 141 (38), 15423-15432.

16. Song, J.; Li, J.; Li, X.; Xu, L.; Dong, Y.; Zeng, H. Quantum Dot Light-Emitting Diodes Based on Inorganic Perovskite Cesium Lead Halides ($CsPbX_3$). *Adv. Mater.* **2015**, 27 (44), 7162-7167.

17. Karlsson, M.; Yi, Z.; Reichert, S.; Luo, X.; Lin, W.; Zhang, Z.; Bao, C.; Zhang, R.; Bai, S.; Zheng, G.; Teng, P.; Duan, L.; Lu, Y.; Zheng, K.; Pullerits, T.; Deibel, C.; Xu, W.; Friend, R.; Gao, F. Mixed Halide Perovskites for Spectrally Stable and High-Efficiency Blue Light-Emitting Diodes. *Nat. Commun.* **2021**, 12 (1), 361.

18. Kumar, G. S.; Sumukam, R. R.; Murali, B. Quasi-2D Perovskite Emitters: A Boon for Efficient Blue Light-Emitting Diodes. *J. Mater. Chem. C* **2020**, 8 (41), 14334-14347.

19. Cheng, L.; Jiang, T.; Cao, Y.; Yi, C.; Wang, N.; Huang, W.; Wang, J. Multiple-Quantum-Well Perovskites for High-Performance Light-Emitting Diodes. *Adv. Mater.* **2019**, 32 (5), 1904163.

20. Zhang, F.; Lu, H.; Tong, J.; Berry, J. J.; Beard, M. C.; Zhu, K. Advances in Two-Dimensional Organic-Inorganic Hybrid Perovskites. *Energy Environ. Sci.* **2020**, 13 (4), 1154-1186.

21. Byun, J.; Cho, H.; Wolf, C.; Jang, M.; Sadhanala, A.; Friend, R. H.; Yang, H.; Lee, T. W. Efficient Visible Quasi-2D Perovskite Light-Emitting Diodes. *Adv. Mater.* **2016**,

28 (34), 7515-7520.

22. Pang, P.; Jin, G.; Liang, C.; Wang, B.; Xiang, W.; Zhang, D.; Xu, J.; Hong, W.; Xiao, Z.; Wang, L.; Xing, G.; Chen, J.; Ma, D. Rearranging Low-Dimensional Phase Distribution of Quasi-2D Perovskites for Efficient Sky-Blue Perovskite Light-Emitting Diodes. *ACS Nano* **2020**, 14 (9), 11420-11430.

23. Wang, Q.; Wang, X.; Yang, Z.; Zhou, N.; Deng, Y.; Zhao, J.; Xiao, X.; Rudd, P.; Moran, A.; Yan, Y.; Huang, J. Efficient Sky-Blue Perovskite Light-Emitting Diodes via Photoluminescence Enhancement. *Nat. Commun.* **2019**, 10 (1), 5633.

24. Liu, Y.; Cui, J. Y.; Du, K.; Tian, H.; He, Z. F.; Zhou, Q. H.; Yang, Z. L.; Deng, Y. Z.; Chen, D.; Zuo, X. B.; Ren, Y.; Wang, L.; Zhu, H. M.; Zhao, B. D.; Di, D. W.; Wang, J. P.; Friend, R. H.; Jin, Y. Z. Efficient Blue Light-Emitting Diodes Based on Quantum-Confined Bromide Perovskite Nanostructures. *Nat. Photonics* **2019**, 13 (11), 760-764.

25. Chu, Z.; Zhao, Y.; Ma, F.; Zhang, C.-X.; Deng, H.; Gao, F.; Ye, Q.; Meng, J.; Yin, Z.; Zhang, X.; You, J. Large Cation Ethylammonium Incorporated Perovskite for Efficient and Spectra Stable Blue Light-Emitting Diodes. *Nat. Commun.* **2020**, 11 (1), 4165.

26. Shang, Y.; Liao, Y.; Wei, Q.; Wang, Z.; Xiang, B.; Ke, Y.; Liu, W.; Ning, Z. Highly Stable Hybrid Perovskite Light-Emitting Diodes Based on Dion-Jacobson Structure. *Sci. Adv.* **2019**, 5 (8), eaaw8072.

27. Yuan, S.; Wang, Z. K.; Xiao, L. X.; Zhang, C. F.; Yang, S. Y.; Chen, B. B.; Ge, H. T.; Tian, Q. S.; Jin, Y.; Liao, L. S. Optimization of Low-Dimensional Components of Quasi-2D Perovskite Films for Deep-Blue Light-Emitting Diodes. *Adv. Mater.* **2019**, 31

(44), 1904319.

28. Lu, J. F.; Jiang, L. C.; Li, W.; Li, F.; Pai, N. K.; Scully, A. D.; Tsai, C. M.; Bach, U.; Simonov, A. N.; Cheng, Y. B.; Spiccia, L. Diammonium and Monoammonium Mixed-Organic-Cation Perovskites for High Performance Solar Cells with Improved Stability. *Adv. Energy Mater.* **2017**, 7 (18), 1700444.

29. Cheng, L.; Liu, Z.; Li, S.; Zhai, Y.; Wang, X.; Qiao, Z.; Xu, Q.; Meng, K.; Zhu, Z.; Chen, G. Highly Thermostable and Efficient Formamidinium-Based Low-Dimensional Perovskite Solar Cells. *Angew. Chem. Int. Ed.* **2020**, 6 (2), 856-864.

30. Wang, H.; Dou, Y.; Shen, P.; Kong, L.; Yuan, H.; Luo, Y.; Zhang, X.; Yang, X. Molecule-Induced P-Doping in Perovskite Nanocrystals Enables Efficient Color-Saturated Red Light-Emitting Diodes. *Small* **2020**, 16 (20), 2001062.

31. Zeng, S.; Shi, S.; Wang, S.; Xiao, Y. Mixed-Ligand Engineering of Quasi-2D Perovskites for Efficient Sky-Blue Light-Emitting Diodes. *J. Mater. Chem. C* **2020**, 8 (4), 1319-1325.

32. Li, N.; Song, L.; Jia, Y.; Dong, Y.; Xie, F.; Wang, L.; Tao, S.; Zhao, N. Stabilizing Perovskite Light-Emitting Diodes by Incorporation of Binary Alkali Cations. *Adv. Mater.* **2020**, 32 (17), 1907786.

33. Quan, L. N.; Zhao, Y.; Garcia de Arquer, F. P.; Sabatini, R.; Walters, G.; Voznyy, O.; Comin, R.; Li, Y.; Fan, J. Z.; Tan, H.; Pan, J.; Yuan, M.; Bakr, O. M.; Lu, Z.; Kim, D. H.; Sargent, E. H. Tailoring the Energy Landscape in Quasi-2D Halide Perovskites Enables Efficient Green-Light Emission. *Nano Lett.* **2017**, 17 (6), 3701-3709.

34. Li, Z.; Chen, Z.; Yang, Y.; Xue, Q.; Yip, H. L.; Cao, Y. Modulation of

Recombination Zone Position for Quasi-Two-Dimensional Blue Perovskite Light-Emitting Diodes with Efficiency Exceeding 5%. *Nat. Commun.* **2019**, 10 (1), 1027.

35. Zhao, L.; Roh, K.; Kacmoli, S.; Al Kurdi, K.; Jhulki, S.; Barlow, S.; Marder, S. R.; Gmachl, C.; Rand, B. P. Thermal Management Enables Bright and Stable Perovskite Light-Emitting Diodes. *Adv. Mater.* **2020**, 32 (25), 2000752.

36. Liu, Y.; Cai, L.; Xu, Y.; Li, J.; Qin, Y.; Song, T.; Wang, L.; Li, Y.; Ono, L. K.; Qi, Y. B.; Sun, B. In-Situ Passivation Perovskite Targeting Efficient Light-Emitting Diodes via Spontaneously Formed Silica Network. *Nano Energy* **2020**, 78, 105134.